J|A|C|S ARTICLES

Published on Web 11/02/2009

Coupling of Triamines with Diisocyanates on Au(111) Leads to the Formation of Polyurea Networks

Sean Jensen, Herbert Früchtl, and Christopher J. Baddeley*

EaStCHEM School of Chemistry, University of St Andrews, North Haugh, St Andrews, Fife, KY16 9ST, United Kingdom

Received May 27, 2009; E-mail: cjb14@st-and.ac.uk

Abstract: The surface-confined coupling reaction between melamine (1,3,5-triazine-2,4,6-triamine) and 1,4-phenylene diisocyanate has been investigated on Au(111) by scanning tunneling microscopy. Diisocyanate species are stabilized at the edges of melamine arrays and coupling reactions to form small urea oligomers may be initiated at room temperature. These oligomers are incorporated into the two-dimensional melamine array. Annealing accelerates the formation of larger oligomers with multiple urea linkages. The oligomers can themselves form ordered 2-D structures stabilized by intermolecular H-bonding. At higher annealing temperatures, oligomers containing as many as seven or eight urea linkages were identified. These oligomers were able to form 2-D porous structures via interoligomer H-bonding interactions. We discuss the composition of all of the phases observed and identify how covalent and noncovalent interactions stabilize each phase.

Introduction

Over the past decade, a vast array of ordered two-dimensional supramolecular structures have been identified on a range of surfaces. Noncovalent interactions comprising hydrogen bonds,[1−5] van der Waals interactions,[6] and metal−organic coordination[3,7,8] have been utilized in the fabrication of such nanoscale architectures.

Though examples have been reported of nanoporous supramolecular networks that are capable of hosting guest species,[1,6,9,10] the chemical and thermal stability of such networks may be insufficient for more widespread use in applications such as templating or catalysis. A strongly preferred alternative would be to fabricate 2-D nanostructures via the formation of covalent linkages on surfaces. However, it is only very recently that covalent reactions have been employed in the formation of 2-D nanostructures on surfaces with the goal of creating extended structurally defined, periodic structures of superior robustness and rigidity.[11−14] Surface-confined thermally induced polymerizations via debromination of porphyrins[15] or 1,3,5-tris(4-bromophenyl)benzene,[16] via condensation reactions between aldehydes and amines[17] and between anhydrides and amines,[18,19] and via nucleophilic attack of acyl chlorides by amines[20] and of *N*-heterocyclic compounds via carbene intermediates[21] have recently been reported. The surface can be used to promote two-dimensional (2-D) polymerization reactions as has been demonstrated by Lipton-Duffin and co-workers who report examples of Ullmann coupling reactions of diiodobenzene on Cu(110),[22] while it is proposed that the surface may be vital to the mechanisms of other unusual reactions such as the conversion of octylamine to trioctylamine on Au(111)[23] and the formation of multiporphyrins on Cu(110).[24]

Isocyanates are an important class of compound. They are key to the formation of polyurethanes and polyureas, two types

(1) Theobald, J. A.; Oxtoby, N. S.; Phillips, M. A.; Champness, N. R.; Beton, P. H. *Nature* **2003**, *424*, 1029.
(2) Kudernac, T.; Lei, S. B.; Elemans, J.; De Feyter, S. *Chem. Soc. Rev.* **2009**, *38*, 402.
(3) Barth, J. V. *Annu. Rev. Phys. Chem.* **2007**, *58*, 375.
(4) De Feyter, S.; Miura, A.; Yao, S.; Chen, Z.; Wurthner, F.; Jonkheijm, P.; Schenning, A.; Meijer, E. W.; De Schryver, F. C. *Nano Lett.* **2005**, *5*, 77.
(5) De Feyter, S.; De Schryver, F. C. *J. Phys. Chem. B* **2005**, *109*, 4290.
(6) Furukawa, S.; Tahara, K.; De Schryver, F. C.; Van der Auweraer, M.; Tobe, Y.; De Feyter, S. *Angew. Chem., Int. Ed.* **2007**, *46*, 2831.
(7) Stepanow, S.; Lingenfelder, M.; Dmitriev, A.; Spillman, H.; Delvigne, E.; Lin, N.; Deng, X.; Cai, C.; Barth, J. V.; Kern, K. *Nat. Mater.* **2004**, *3*, 229.
(8) Lin, N.; Stepanow, S.; Ruben, M.; Barth, J. V. Surface-Confined Supramolecular Coordination Chemistry. In *Templates in Chemistry Iii*; Springer-Verlag: Berlin, 2009; Vol. 287, p 1.
(9) Theobald, J. A.; Oxtoby, N. S.; Champness, N. R.; Beton, P. H.; Dennis, T. J. S. *Langmuir* **2005**, *21*, 2038.
(10) Madueno, R.; Raisanen, M. T.; Silien, C.; Buck, M. *Nature* **2008**, *454*, 618.
(11) Gourdon, A. *Angew. Chem., Int. Ed.* **2008**, *47*, 6950.
(12) Champness, N. R. *Nat. Nanotechnol.* **2007**, *2*, 671.
(13) Sakamoto, J.; van Heijst, J.; Lukin, O.; Schluter, A. D. *Angew. Chem., Int. Ed.* **2009**, *48*, 1030.
(14) Perepichka, D. F.; Rosei, F. *Science* **2009**, *323*, 216.
(15) Grill, L.; Dyer, M.; Lafferentz, L.; Persson, M.; Peters, M. V.; Hecht, S. *Nat. Nanotechnol.* **2007**, *2*, 687.
(16) Gutzler, R.; Walch, H.; Eder, G.; Kloft, S.; Heckl, W. M.; Lackinger, M. *Chem. Commun.* **2009**, 4456.
(17) Weigelt, S.; Busse, C.; Bombis, C.; Knudsen, M. M.; Gothelf, K. V.; Strunskus, T.; Woll, C.; Dahlbom, M.; Hammer, B.; Laegsgaard, E.; Besenbacher, F.; Linderoth, T. R. *Angew. Chem., Int. Ed.* **2007**, *46*, 9227.
(18) Treier, M.; Fasel, R.; Champness, N. R.; Argent, S.; Richardson, N. V. *Phys. Chem. Chem. Phys.* **2009**, *11*, 1209.
(19) Treier, M.; Richardson, N. V.; Fasel, R. *J. Am. Chem. Soc.* **2008**, *130*, 14054.
(20) Schmitz, C. H.; Ikonomov, J.; Sokolowski, M. *J. Phys. Chem. C* **2009**, *113*, 11984.
(21) Matena, M.; Riehm, T.; Stohr, M.; Jung, T. A.; Gade, L. H. *Angew. Chem., Int. Ed.* **2008**, *47*, 2414.
(22) Lipton-Duffin, J. A.; Ivasenko, O.; Perepichka, D. F.; Rosei, F. *Small* **2009**, *5*, 592.

10.1021/ja9043032 CCC: $40.75

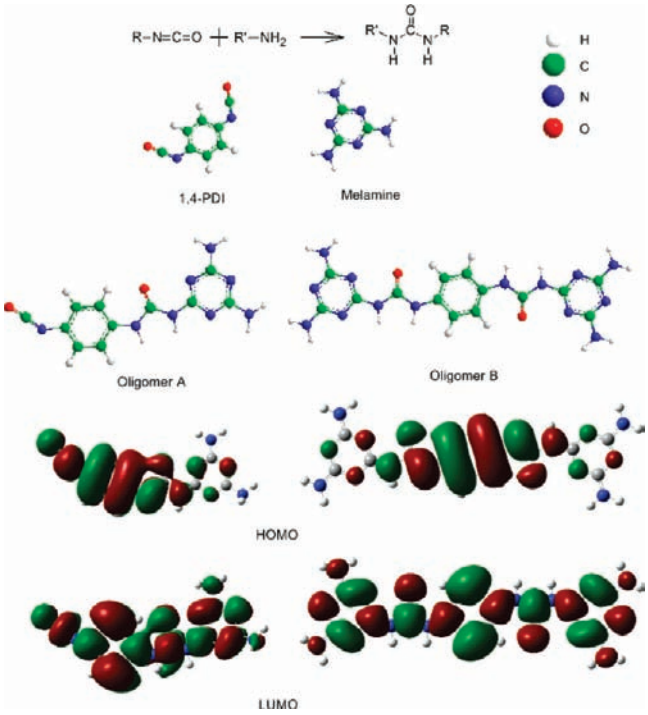

Figure 1. Coupling reaction between an isocyanate and an amine. The molecular structures of melamine, 1,4-phenylene diisocyanate, and two short oligomer products, A and B, are shown with calculated HOMOs and LUMOs (Gaussian 03, density functional theory using M05-2X functional with 6-311+g* basis set) below the respective oligomer product. The frontier orbitals depicted were calculated at the molecular geometry on the surface.

of polymer that have huge ranges of applications such as foams, coatings, and adhesives. The isocyanate group (−N=*C*=O) is particularly reactive to compounds that contain a mobile hydrogen atom of the type X−H and addition reactions typically occur at the N=C bond[25] (Figure 1). Amine groups react with isocyanate groups to produce urea compounds; these reactions often take place readily in solution at room temperature. Furthermore, it is well-established that a diisocyanate can react with a polyamine to produce a polyurea. The urea linkage (−NH−CO−NH−) itself is highly useful because it contains three bonds amenable to hydrogen bonding and it is vital in many systems that rely upon molecular recognition.[26]

In this study, we investigate, with the use of scanning tunneling microscopy (STM) in ultrahigh vacuum (UHV), the formation of a polyurea network on Au(111). A primary aim of the work is to form 2-D covalently bonded networks with a defined functionality that can later be utilized in molecular recognition in applications such as (enantio)selective catalysis or (bio)sensors. Studies of isocyanate/amine-coupling reactions at surfaces have been carried out at or near room temperature, in both UHV-[27] and solution[28−30]-based environments with the aim of producing 3-D urea structures. Here, we show that the coupling reaction can take place between a diisocyanate adsorbate, 1,4-phenylene diisocyanate (1,4-PDI), and a triamine adsorbate, 1,3,5-triazine-2,4,6-triamine (melamine), in two dimensions on the Au(111) surface and discuss the novel network structures that are formed by the reaction. On Au(111), melamine forms a distinctive hexagonal structure that is stabilized by hydrogen bonding; two N−H···N interactions exist between each molecule at every melamine−melamine junction within the arrangement.[31,32] We discuss the temperature dependent transformation of this structure and conclude that the changes observed are due to the formation of oligomers containing multiple urea linkages.

Experimental Section

The STM experiments were carried out in an Omicron UHV system with a base pressure of 1×10^{-10} mbar. The Au(111) sample was prepared by cycles of argon ion bombardment (1 kV) and annealing to 873 K until low-energy electron diffraction and STM indicated the presence of a clean Au(111) surface, exhibiting the characteristic ($\sqrt{3} \times 22$) herringbone reconstruction.[33] Melamine (Sigma-Aldrich) was heated to 363 K and sublimed onto the Au(111) substrate, which was held at 300 K. 1,4-Phenylene diisocyanate (Sigma-Aldrich) was sublimed by heating to 333 K. Images of the surface were acquired by transfer under UHV conditions to the STM chamber where data were taken in constant current mode using an electrochemically etched W tip. All STM images were acquired at room temperature. STM images were processed using WSxM software.[34]

Simulations

Simulations on the isolated molecules were carried out with Gaussian 03,[35] employing density functional theory (DFT) using the M05-2X meta-generalized gradient approximation functional[36] and 6-311+g* basis set.[37] The proposed phases on the gold surface were modeled by periodic DFT calculations using the SIESTA program,[38] employing the Perdew−Burke−Ernzerhof functional,[39] a numerical split-valence pseudoatomic orbital[40] basis set with polarization functions and Troullier-Martin pseudopotentials[41] as available from the SIESTA Web site. Based on the assumption that the geometry of the adsorbate layer is predominantly determined by the H-bond network and other intermolecular interactions rather than chemical interactions with the gold atoms, we modeled only the molecular layer. The effect of the Au surface was simulated by constraining all carbon atoms into a plane. This allowed us to optimize the cell geometries based on the intermolecular interac-

(23) Weigelt, S.; Schnadt, J.; Tuxen, A. K.; Masini, F.; Bombis, C.; Busse, C.; Isvoranu, C.; Ataman, E.; Laegsgaard, E.; Besenbacher, F.; Linderoth, T. R. *J. Am. Chem. Soc.* **2008**, *130*, 5388.
(24) Veld, M. I.; Iavicoli, P.; Haq, S.; Amabilino, D. B.; Raval, R. *Chem. Commun.* **2008**, 1536.
(25) Caraculacu, A. A.; Coseri, S. *Prog. Polym. Sci.* **2001**, *26*, 799.
(26) Etter, M. C.; Urbanczyklipkowska, Z.; Ziaebrahimi, M.; Panunto, T. W. *J. Am. Chem. Soc.* **1990**, *112*, 8415.
(27) Kim, A.; Filler, M. A.; Kim, S.; Bent, S. F. *J. Am. Chem. Soc.* **2005**, *127*, 6123.
(28) Kohli, P.; Blanchard, G. J. *Langmuir* **2000**, *16*, 4655.
(29) Vogel, B. M.; DeLongchamp, M.; Mahoney, C. M.; Lucas, L. A.; Fischer, D. A.; Lin, E. K. *Appl. Surf. Sci.* **2008**, *254*, 1789.
(30) van Gorp, J. J.; Vekemans, J.; Meijer, E. W. *J. Am. Chem. Soc.* **2002**, *124*, 14759.
(31) Perdigao, L. M. A.; Perkins, E. W.; Ma, J.; Staniec, P. A.; Rogers, B. L.; Champness, N. R.; Beton, P. H. *J. Phys. Chem. B* **2006**, *110*, 12539.
(32) Silly, F.; Shaw, A. Q.; Castell, M. R.; Briggs, G. A. D.; Mura, M.; Martsinovich, N.; Kantorovich, L. *J. Phys. Chem. C* **2008**, *112*, 11476.
(33) Barth, J. V.; Brune, H.; Ertl, G.; Behm, R. J. *Phys. Rev. B* **1990**, *42*, 9307.
(34) Horcas, I.; Fernandez, R.; Gomez-Rodriguez, J. M.; Colchero, J.; Gomez-Herrero, J.; Baro, A. M. *Rev. Sci. Instrum.* **2007**, *78*, 8.
(35) Frisch, M. J., et al. *Gaussian 03*, revision E.0; Gaussian, Inc.: Wallingford, CT, 2004.
(36) Zhao, Y.; Schultz, N. E.; Truhlar, D. G. *J. Chem. Theor. Comput.* **2006**, *2*, 364.
(37) Krishnan, R.; Binkley, J. S.; Seeger, R.; Pople, J. A. *J. Chem. Phys.* **1980**, *72*, 650.
(38) Soler, J. M.; Artacho, E.; Gale, J. D.; Garcia, A.; Junquera, J.; Ordejon, P.; Sanchez-Portal, D. *J. Phys.: Condens. Matter* **2002**, *14*, 2745.
(39) Perdew, J. P.; Burke, K.; Ernzerhof, M. *Phys. Rev. Lett.* **1996**, *77*, 3865.
(40) Sankey, O. F.; Niklewski, D. J. *Phys. Rev. B* **1989**, *40*, 3979.
(41) Troullier, N.; Martins, J. L. *Phys. Rev. B* **1991**, *43*, 1993.

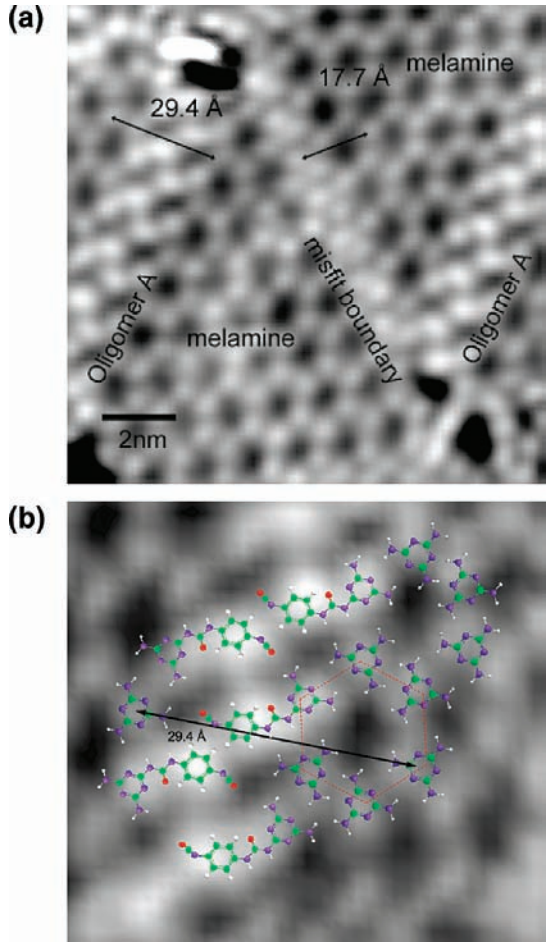

Figure 2. (a) STM image comparing the misfit boundaries in melamine domains with those caused by the incorporation of 1,4-PDI and possible formation of Oligomer A (12.9 × 12.9 nm, 1.5 V, 0.2 nA). (b) Model showing the proposed packing of Oligomer A species at the boundary of two domains of melamine on Au(111).

tions. The unit cell length orthogonal to the plane of the molecular network was kept at 20 Å; all other lattice parameters were optimized. Intermolecular interaction energies quoted are counterpoise corrected.

Results and Discussion

Following the deposition of melamine and, subsequently, 1,4-PDI onto the clean Au(111) surface, initially held at room temperature, only the characteristic hexagonal melamine arrangement, which we will refer to as phase I, is observed (Figure 2a); each melamine molecule is typically observed, under conditions of good resolution, as a single triangular feature because of the location and shape of its molecular orbitals.[42] This arrangement is stabilized by double hydrogen bonds between adjacent molecules and is discussed in more detail elsewhere.[31,32]

Definitive single-component arrangements of 1,4-PDI on Au(111) are not observed under these conditions. This may be explained by a high diffusion rate rendering the species invisible to STM at room temperature or the species may exhibit too low a sticking probability on Au(111) at 300 K. To enhance the sticking probability of 1,4-PDI, melamine was first deposited on the surface. Subsequent changes in the appearance of melamine domains after a few hours were the only indication of the presence of 1,4-PDI on the surface.

Figure 2a shows that striped features are observed between domains of pure melamine. The features within these stripes appear brighter than melamine molecules and the features are less densely packed than those in the typical misfit domain boundaries identified by Silly et al.[32] A distance of 29.4 Å is measured between the centers of molecules in equivalent positions within the two hexagonal arrangements on either side of the boundary (Figure 2b). The analogous distance across the boundaries discussed by Silly et al. is only 17.69 Å.[32] This additional distance may be explained by the formation of a mixed, unreacted domain of melamine and 1,4-PDI; the new features appear bolder than the bulk of the melamine domain and the shortest center-to-center distance between the bright regions of the features is 8.5 Å, which is longer than the typical center-to-center separation between melamine molecules of 6.1 Å.[31] The new feature could also be explained by the incorporation of Oligomer A (Figure 1), created by the reaction of a single melamine with a single 1,4-PDI molecule to produce monosubstituted melamine units consisting of two aromatic rings (IUPAC nomenclature: 1-(4,6-diamino-1,3,5-triazin-2-yl)-3-(4-isocyanatophenyl) urea). The total distance across the two bright features that give rise to the aforementioned 8.5 Å center-to-center separation is measured as 15.2 Å, which is comparable to the length of Oligomer A of 15.3 Å calculated using DFT (M05-2X/6-311g*). The triazine part of Oligomer A retains two amino substituents and can thus be incorporated as part of a melamine hexagon. The remainder of the molecule, with its isocyanate terminus, is seen to interlock with like molecules protruding from the other side of the boundary and the arrangement may be stabilized by hydrogen bonds between the isocyanate C═O bonds and the N−H bonds on adjacent species. Similarly, wider domain boundaries are sometimes observed. The species linking the two domains may be a second oligomer (IUPAC name: 1,1-(1,4-phenylene)bis(3-(4,6-diamino-1,3,5-triazin-2-yl), Oligomer B (Figure 1, to be discussed later), which contains two urea functionalities and can participate in the formation of melamine-type hydrogen-bonding hexagons and hydrogen-bond to the simple melamine-phenylene isocyanate urea oligomers at each terminus. Hence, like Oligomer A, it is readily understandable how Oligomer B is also capable of undergoing incorporation into the melamine domains.

Once certain that 1,4-PDI is present as an adsorbate, the surface may be annealed to accelerate polymerization; it is thought that the main purpose of the annealing treatments is to create space for reactions to occur by perturbation of dense supramolecular arrangements rather than to activate the addition reaction.

Figure 3a shows a new porous phase, phase II, of which domains (100 × 100 nm) are observed after annealing the surface to 345 K. The new phase has a rectangular unit cell with lattice constants of 40.8 × 46.4 Å, where the longer side is orientated at 40° to the <$\bar{1}\bar{1}$2> direction. We interpret phase II as consisting of Oligomer A and melamine in a 3:1 ratio. The spatial distribution of highest occupied molecular orbitals (HOMO) and lowest occupied molecular orbitals (LUMO) of Oligomers A and B were calculated using Gaussian 03 software and are shown in Figure 1. Adsorbed molecules may be expected to have a comparable shape in STM images. On this basis, it is believed that the features, which measure 15.2 Å in length and appear as two connected lobes, correspond to Oligomer A, while as aforementioned, melamine appears as singular triangular

(42) Chis, V.; Mile, G.; Stiufiuc, R.; Leopold, N.; Oltean, M. *J. Mol. Struct.* **2009**, *47*, 924–926.

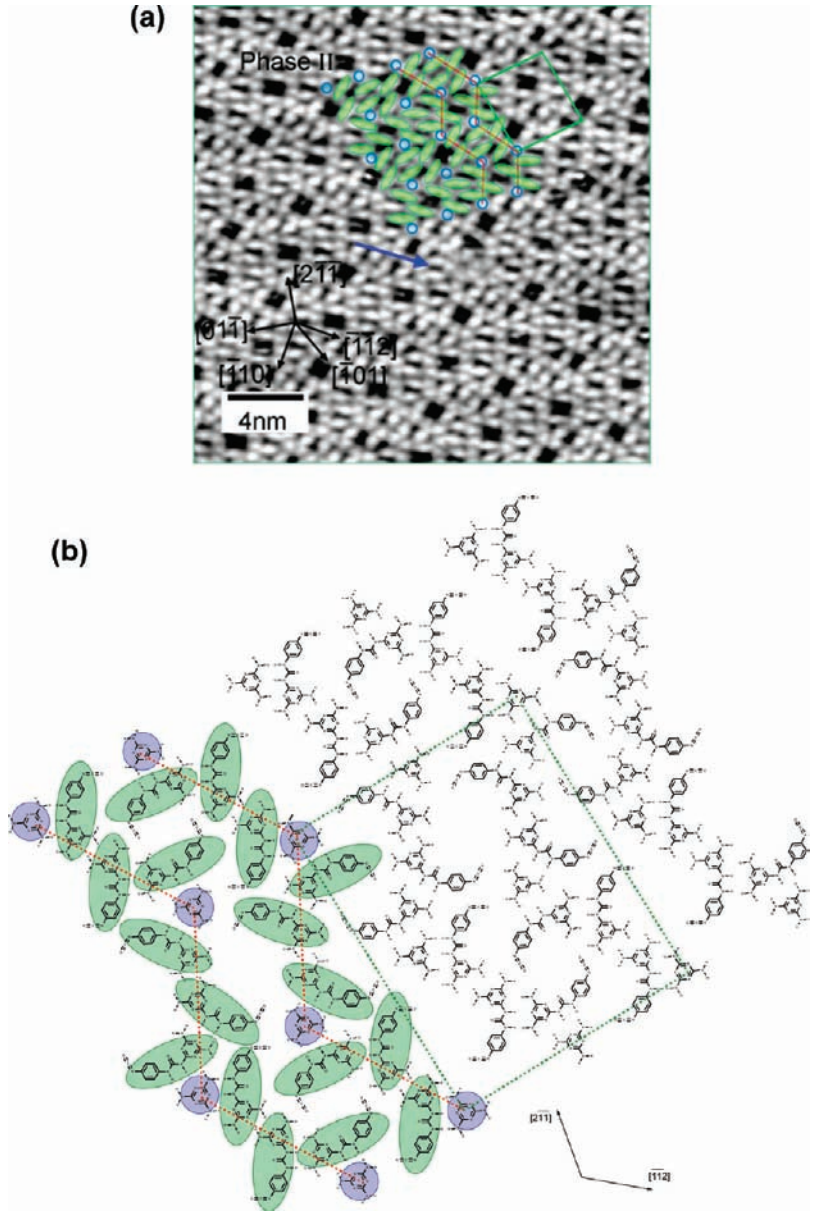

Figure 3. (a) STM image of phase II consisting of melamine and Oligomer A created after the surface is annealed to 345 K (23 × 23 nm, 1.5 V, 0.35 nA). The red zigzags highlight the herringbone pattern made up of triazine moieties that run throughout the phase. The blue arrow points toward one of the many defects: two complete hexagon arrangements of unreacted melamine molecules. (b) Schematic diagram showing the molecular packing in the porous Oligomer A:melamine network, phase II.

features. Under the imaging conditions used (i.e., tip biased positively), one would anticipate that the imaged molecule may resemble the HOMO in appearance with electrons being transferred from filled sample states to empty tip states. In general, when imaged under these conditions, the triazine moiety of Oligomer A is observed as triangular, the features narrow close to the middle where the urea linkage exists, and it is presumed that elongated STM features represent the aromatic isocyanate fixed to melamine via a urea linkage; the triangular shape is consistent with the appearance of melamine, while the brighter portion of the feature reflects the greater electron density on the aromatic isocyanate moiety. The structure is constructed from a series of parallel zigzags running approximately along the <$\bar{1}\bar{1}$2> type directions of the surface. We interpret the structure as containing an unreacted melamine molecule at the vertex of each zigzag. The 120° rotation in the alignment of features along the zigzag is caused by the threefold symmetry of the melamine molecule. Between two vertices of the zigzag, two elbow-located melamine features are separated by three features of similar appearance. The length of the line segment of the zigzag is 24.6 Å, which is equivalent to four center-to-center spacings in the typical melamine monolayer arrangement. We conclude that the three features connecting the two isolated melamine molecules at each vertex are the triazine units of Oligomer A species connected via typical melamine−melamine N−H---N hydrogen bonds. The phenyl isocyanate moieties of each of these species extend into the interim space like branches. It appears that adjacent zigzags interlock with each other via several different types of hydrogen-bonding arrangements between isocyanate groups and amine groups of neighboring zigzags. The steric hindrance associated with the phenylisocyanato moieties of Oligomer A disfavors the formation of a third H-bonding interaction between a melamine species and a triazine unit; instead, the isolated melamine species form the corners

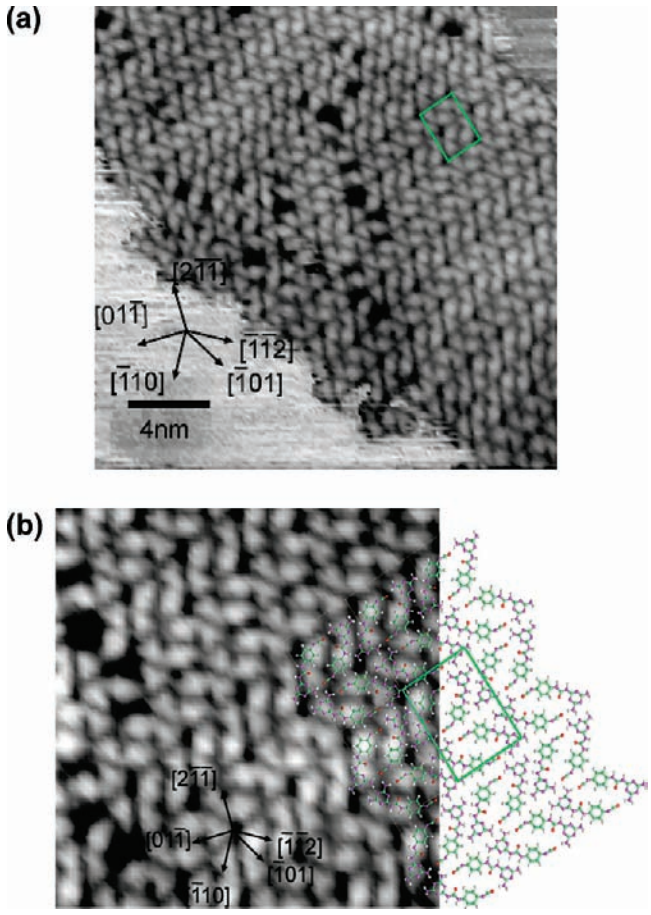

Figure 4. (a) STM image of phase III, consisting of Oligomer A (21 × 21 nm, 1.5 V, 0.35 nA). (b) Schematic model of phase III. The superimposed model has the dimensions of the energy-minimized unit cell.

of rectangular pores of approximate dimensions 10 × 8 Å. There are a number of defects in the domain. Close to the center of Figure 3a (indicated by an arrow), one may observe a defect in the domain which consists of two adjacent hexagons of melamine units. In other areas the rectangular porous structure is lost. Presumably, there is some flexibility in the orientation of Oligomer A, leading to the formation of defects in the structure.

Annealing the surface to 360 K results in the formation of a new phase (phase III, Figure 4a) consisting exclusively of Oligomer A in an ordered arrangement. Once formed, phase III is dominant up to 420 K, although it must be noted that as the temperature is increased throughout this range, the abundance of features caused by the presence of larger oligomers also increases. Figure 4b displays a more detailed image of phase III on which is superimposed the energy-minimized model structure. Phase III has a rectangular unit cell, of sides ~23.8 and ~18.0 Å, with the longer side orientated at 40° to the <$\bar{1}\bar{1}$2> direction or its equivalents; the unit cell matches the values 23.12 and 16.74 Å for the model calculated within reasonable error.

Within phase III, pairs of Oligomer A align to promote the formation of a number of intermolecular hydrogen bonds. Each Oligomer A species forms four hydrogen bonds with the parallel oligomer. In the energy-minimized structure each of these N−H---N distances fall in the range 2.8−3.0 Å, which is consistent with H-bond lengths. Two of these involve N−H···N interactions between the urea N−H bonds and the triazine. In the energy-minimized model an additional two hydrogen bonds are possible between urea N−H and one of the unreacted $-NH_2$ functionalities of the triazine of the neighboring molecule. In the latter case, these two hydrogen bonds require the two N−H bonds of the NH_2 functionality to rotate out of the plane of the molecule. Additional stabilization is achieved via hydrogen bonds between the −NCO functionality and $-NH_2$ groups on neighboring molecules. Alternate rows are almost related by mirror symmetry, giving the phase a "herringbone" appearance. There is a small offset that breaks the mirror symmetry. The offset allows the optimization of intermolecular H-bonding interactions.

The energy-minimized structure of an isolated Oligomer A molecule is found not to be perfectly planar. The energy cost associated with the molecule adopting a planar geometry and thereby optimizing intermolecular interactions and substrate−molecule interactions is, however, only ~0.03 eV. The calculated 2-D structure is stabilized by 0.76 eV per molecule compared with the isolated planar molecule. One would anticipate additional stabilization of a similar magnitude if the interaction between the molecule and the surface was also considered.

This phase shows remarkable stability in light of the fact that reactive groups are still abundant within its arrangement and in very close proximity on the surface. The slow rate of reaction can be attributed not only to the steric hindrance provided by the substrate, which inhibits nucleophilic attack, but also to the close packing, aided by the formation of a large number of intermolecular hydrogen bonds, in the initial melamine phase and subsequently in the phases II and III, both of which presumably prevent molecules that possess amine and isocyanate groups from adopting favorable positions for reaction.

Double addition to 1,4-PDI by two melamine molecules leads to the formation of diurea oligomers, Oligomer B, containing three aromatic rings and including two urea linkages (IUPAC nomenclature: 1,1′-(1,4-phenylene)bis(3-(4,6-diamino-1,3,5-triazin-2-yl)urea)). These oligomers can assemble into porous formations such as those observed in Figure 4a and Figure 5a (Phase IV). Oligomer B is observed as features of three connected lobes; as with Oligomer A and the comparable HOMO and LUMO models of Figure 1, the triazine moieties appear as triangular lobes, the features are narrower close to the urea linkages on either side of the middle phenyl ring which, because of a higher electron density, typically appears brighter than the triazine rings. Throughout the temperature range at which phase III is stable (360 K ≤ T ≤ 420 K), smaller domains of these molecules are observed that are often present at the outermost edge of phase III. This is consistent with the concept of close-packed domains on the surface hindering the urea-forming reaction; these structures are still observed after annealing to around 520 K. Figure 5b shows a model of the porous rectangular arrangement formed by these oligomers. The measured unit cell for this structure has sides separated by an angle of ~30°, of 19.9 Å and 16.7 Å; this is in close agreement with the calculated dimensions of 20.15 and 17.18 Å for the calculated model of phase IV as shown superimposed on a zoomed STM image in Figure 5b. The shorter side of the unit cell can be seen as closely aligned with the <$\bar{1}\bar{1}$2> direction or its equivalents. The measured center-to-center spacing between triazine rings at the junctions is ~6.2 Å, which is consistent with the melamine−melamine-type stabilization by hydrogen bonding at the junctions where the equivalent distance is 6.1 Å. The rhombic pores are measured to be around 4 Å wide.

Figure 5c shows phase V, a Kagomé lattice formed from Oligomer B near the edges of a compact domain of Oligomer

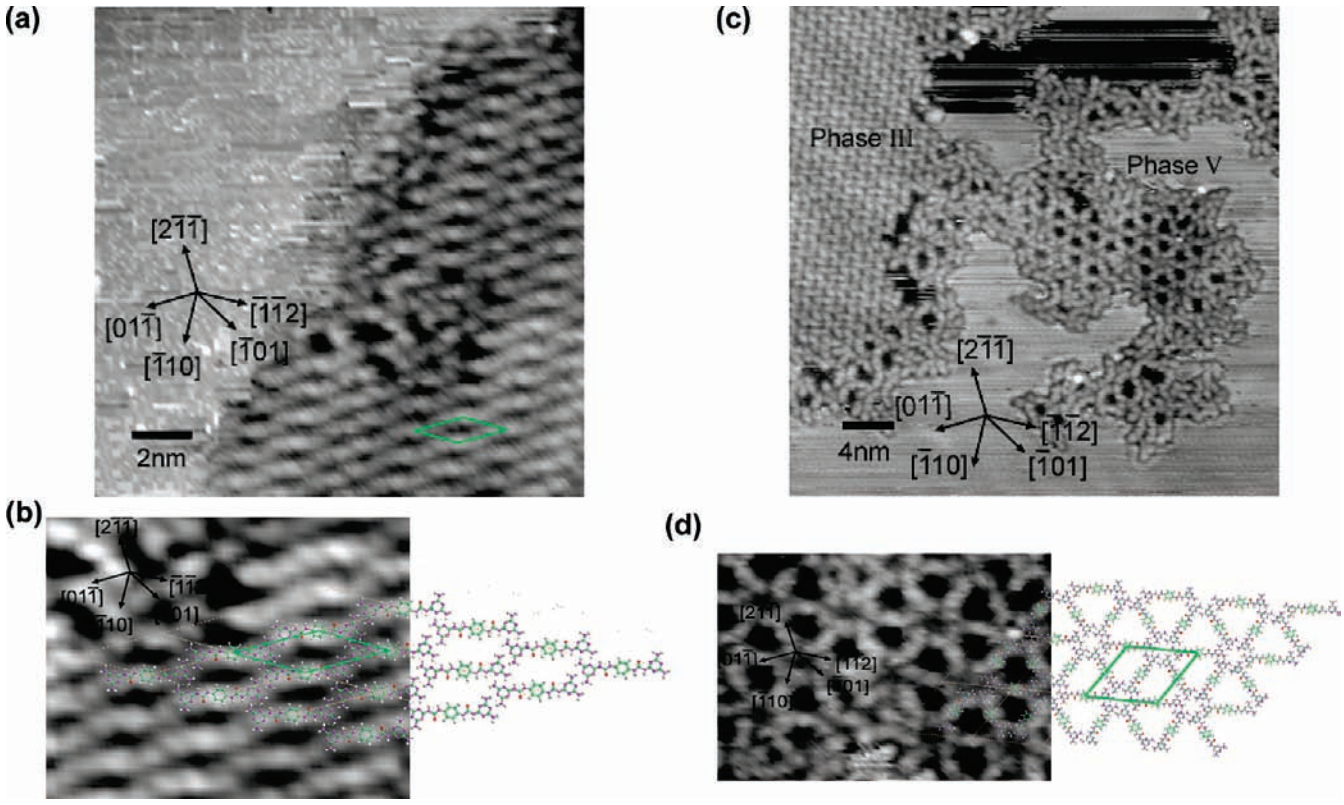

Figure 5. (a) STM image showing porous rectangular phase IV formed from Oligomer B at the edge of a domain after annealing to 350 K (16.3 × 16.3 nm, 1.5 V, 0.35 nA). (b) Schematic model of the porous rectangular phase IV of Oligomer B. (c) STM image showing the Kagome arrangement of Oligomer B, phase V, beside a domain of phase III after the surface was annealed to 420 K (38.3 × 38.3 nm, 1.5 V, 0.5 nA). (d) Model of the Kagome arrangement of Oligomer B, phase V.

A after annealing the surface to 420 K. Shown in more detail in Figure 5d, this feature is observed quite frequently between 420 and 490 K, a temperature range where widespread disruption of the herringbone phase and formation of larger oligomers is observed. On the basis of prior knowledge of the stabilization of the melamine arrangement on Au(111), the Kagomé lattice can be explained simply as follows. The arrangements are based on a hexagonal center that consists of the diamino triazine moieties of six Oligomers B in an arrangement structurally identical to the hexagonal arrangement formed by six melamine molecules within their typical hydrogen-bonding arrangement.[32] It is noteworthy that, as such, the Kagomé lattice formed here is inherently chiral. A given hexagon is linked to six other hexagons via two new urea linkages on either side of phenyl moieties. The unit cell of this arrangement has sides of ~27.1 Å separated by an angle of 60° and parallel to the <$\bar{1}\bar{1}$2> direction or its equivalents; the measurements are in good agreement with the calculated values of 26.85 Å and 60°, respectively, in our energy-minimized model. Pores with a triangular shape are produced with side ~1 nm. Each pore contains three urea functionalities. Ordered regions of phase V of ~20 × 10 nm were typically identified at the edges of phase III domains; other larger oligomers are seen to surround these domains and sometimes create distortions within them.

Figure 6a shows that the surface after annealing to 520 K is largely characterized by larger molecular weight oligomers. Either through desorption of the smallest oligomers or reaction, complete disappearance of the herringbone phase is realized after annealing to 470 K. The resultant surface arrangements are, on the whole, not well-ordered, apart from areas of phase VI which often bound domains of larger oligomers. These larger oligomers are mostly snake-like chains with each melamine unit in the oligomers having been disubstituted. Hydrogen bonding between the remaining free amine groups and triazine rings along these longer oligomers is most likely responsible for their positioning within these domains; pores that are ~15 Å wide are regularly observed (Figure 6b). The target network of trisubstituted melamine molecules is shown in Figure 6c; this would contain pores ~25 Å wide. Twelve molecules (six of each reactant) would have to bond with the appropriate orientation to form a single pore of this ideal structure. Although some instances of "half pores" (semicircular arrangements of oligomers of six molecules linked as in the ideal structure) are observed, the pores most frequently observed consist of walls consisting of up to nine urea linkages; two nearby oligomers are seen to align such that the pore becomes closed only by two melamine−melamine-type hydrogen-bonding interactions on opposite sides of the pore. One of the advantages of self-assembly is the ability of domains of molecules held together by noncovalent interactions to be able to "self-heal", eliminate defects, and create uniformity; these domains, although controlled largely by hydrogen bonding, are unable to do so largely because of the variation in the sizes of the oligomers that have conglomerated.

The production of fully covalent pores appears to be hindered by the inability of melamine to undergo trisubstitution via reaction with three isocyanate species. In principle, a single covalent pore would be produced by the reaction of six melamine molecules and six 1,4-PDI species whereby each melamine undergoes only two coupling reactions and the twelve molecules arrange in a hexagonal configuration. We found no examples of this type of structure. Instead, snake-like chains containing twelve aromatic rings were widespread.

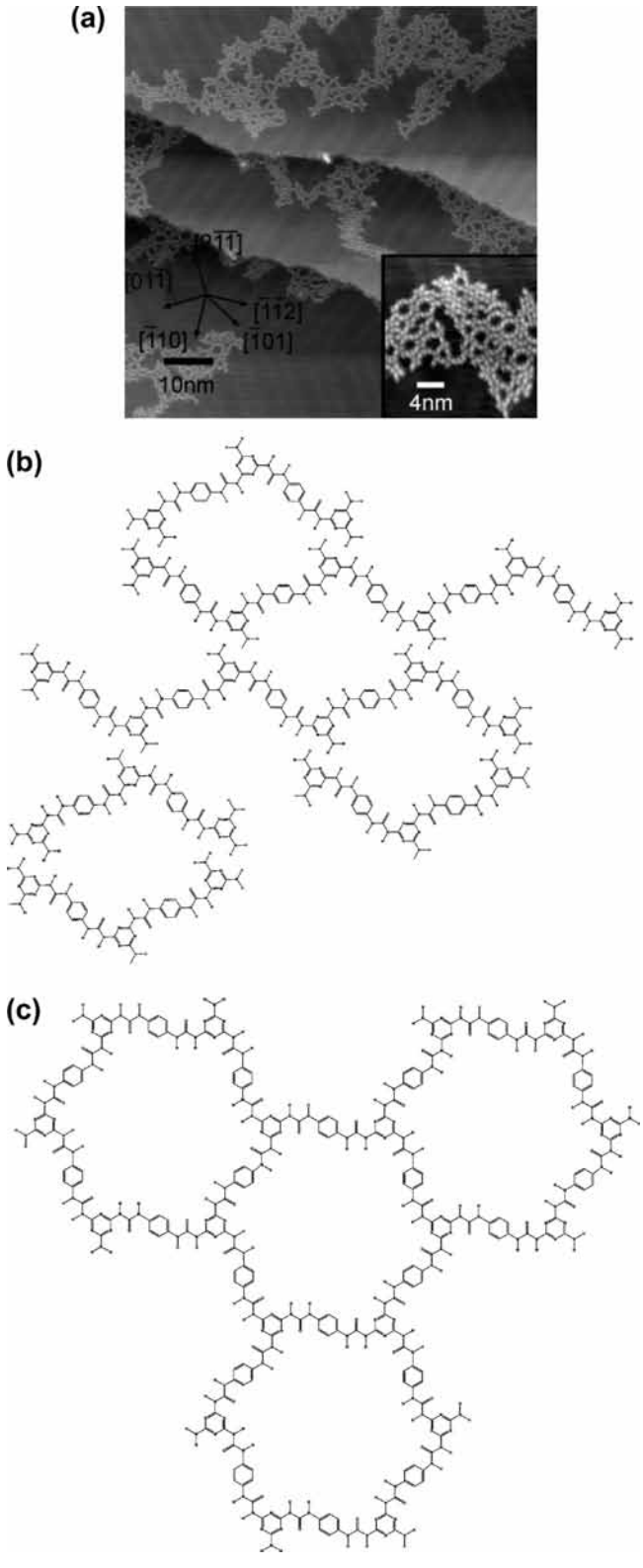

Figure 6. (a) STM image of the surface after annealing to 520 K (90 × 90 nm, 1.5 V, 0.3 nA). Domains of phase IV occasionally emanate from aggregates of polymeric chains. (b) Model showing how longer oligomer chains can interact to create pores. (c) Model showing a small area of the ideal network formed by the trisubstitution of melamine units. This network was not observed in our experiments.

From these observations, it can be deduced that trisubstitution of melamine by aromatic isocyanate molecules (in this case, often larger oligomers) is unfavorable, presumably for either (or both) steric or electronic reasons. As substitution of amino groups for urea substituents occurs on melamine molecules, their remaining amine groups must be progressively deactivated toward reaction; monosubstitution to form Oligomers A and B is observed at lower temperatures while larger oligomers are observed more regularly only as the temperature is increased above 420 K. Formation of large ordered domains of melamine in its close-packed hydrogen-bonding formation further inhibits trisubstitution by blocking the access of 1,4-PDI to the amine functionalities of melamine. Annealing the surface is required to accelerate the reaction and there is considerable evidence that reaction initially occurs only at the edges of ordered H-bonded domains. The initial introduction of order to the surface via the self-assembly of melamine into its hexagonal formation may be key to the formation of subsequent ordered domains such as the porous phase II observed at 350 K and the compact phase III observed from 360 to 470 K; it may be expected that if melamine was less ordered in the initial stages, then polymeric features that begin to be observed from 440 K would be formed at much lower temperatures.

As aforementioned, the highest annealing temperature tested in this series was 520 K, and although some of the smallest oligomers, Oligomer A, may have desorbed from the surface by this temperature, it can be concluded that structures of greater thermal stability on Au(111) than the starting material, melamine, which is known to desorb at around 370 K, were generated by these reactions. The goal of these experiments was to create covalent structures, and although these have been generated, it is remarkable that the same hydrogen-bonding interactions, two N−H···N bonds at each junction, that exist within the two-dimensional melamine array are still largely responsible for the spatial distribution of the much larger oligomers formed during these experiments. Despite the lack of order and the inability to form porous structures of fully covalent pore walls from melamine and 1,4-PDI, the final products of these polymerization reactions may still be capable of performing some tasks where molecular recognition is key due to the presence of the urea linkages and their hydrogen-bonding capabilities.

Conclusions

The reaction between melamine and 1,4-phenylene diisocyanate to produce urea linkages is observed directly via STM. It is possible that the reaction takes place at room temperature at the edge of pure melamine domain—although annealing is required to disrupt some of the close-packed melamine domains (phase I), which are stabilized by supramolecular interactions, and accelerate the polymerization. At lower annealing temperatures, smaller oligomers are observed and these form ordered supramolecular arrangements.

Phase II, a porous, bicomponent phase, consisting of melamine and Oligomer A, is formed from phase I around 345 K, as the abundance of this small oligomer increases. Phase III is a compact, monocomponent phase of Oligomer A, prevalent from 350 to 420 K; this becomes more widespread as the melamine in phase II is displaced or reacted. Phases IV and V consist of Oligomer B; these form on the edges of domains of phase III and become more abundant as the temperature is increased. Finally, only longer oligomeric chains are formed at the highest annealing temperatures, up to 520 K, as the molecules of phase III react or desorb.

The incorporation of functionality into surface nanostructures is highly desirable and although structures of fully covalent pore walls are not observed from melamine and 1,4-phenylene diisocyanate, the formation of the urea functionality within porous 2-D structures represents opportunities for host−guest interactions with further adsorbates, which may be of significance in templating and catalysis.

Acknowledgment. We gratefully acknowledge EPSRC (Basic Technology grant EP/D048761/1) for funding and Professor Neville Richardson for access to his STM instrument. We thank EaStCHEM for support via the EaStCHEM Research Computing Facility.

JA9043032